Morphological equilibration of a facetted crystal

M. Ozdemir and A. Zangwill
School of Physics, Georgia Institute of Technology, Atlanta, Georgia 30332
(Received 9 September 1991)

We study the morphological equilibration of a finite, facetted crystal by use of phenomenological equations of motion. The relevant atomistic kinetic processes (edge transfer, kink attachment and/or detachment, terrace hopping, and surface diffusion) are introduced progressively with special attention given to a proper treatment of the latter. Unlike all previous work, the role of individual step motion (including the effect of step-step interactions) is considered in detail. Approximate analytic results are obtained for two- and three-dimensional model crystals and compared to the work of others. Numerical results for the time dependence of the equilibration and the shape of the crystal during equilibration are presented for a model two-dimensional crystal in various limits of the kinetic parameters. Characteristic behavior is found when the different kinetic processes are individually rate limiting. Although each facet remains flat on macroscopic scales, multiple-step generation is found to lead to interesting microscopic step distributions and equilibration scenarios. The latter might be observable by appropriate microscopies.

I. INTRODUCTION

The problem of predicting the equilibrium shape of a finite crystal has enjoyed sustained theoretical attention for nearly a century[1] and continues to be an active area of research up to the present day.[2] Despite this impetus, there have been relatively few laboratory studies devoted to the problem.[3] In part, this is so because the experimenter must grapple with various problems of *kinetics* before any meaningful statements regarding equilibrium can be made. Indeed, kinetic processes determine both the shape of a crystal as it grows and the rate and manner by which it ultimately achieves its equilibrium form. Curiously, while there has been considerable work directed to the morphological kinetics of crystal growth itself,[4] the kinetics of the transformation of a growth form to an equilibrium form is virtually unstudied. For the particularly interesting case of a *facetted* crystal, there are only a handful of exceptions. Experimental work appears to be confined to the metallurgical literature[5] and existing theoretical studies[6–9] do not provide an explicit account of the principal mechanism of mass transport, i.e., surface diffusion. The purpose of the present paper is to redress this situation and to provide a reasonably complete discussion of the kinetics of morphological equilibration for the case of a finite, facetted crystal.

To appreciate the discussion to follow, it is important to recognize that mass transport at the surface of a facetted crystal is completely different from mass transport at the surface of a nonfacetted crystal. The latter, which corresponds to the case when the surface free energy (surface tension) is an analytic function of crystallographic orientation (an amorphous material or a crystal at a temperature in excess of the relevant roughening[10] temperatures), is well understood.[11] By contrast, when the morphology of a surface is best regarded as a sequence of flat (low-index) terraces separated by monatomic steps, capillary effects are much more difficult to treat. The only problem completely analyzed to date is the morphological equilibration of one isolated crystalline facet perturbed by a small-amplitude corrugation wave.[12,13] Indeed, our interest in the subject of this paper was motivated by our efforts to generalize our previous results[13] to a corrugation wave of large amplitude which exposes inequivalent facets.

We find it convenient to approach this class of problems from the point of view of nonequilibrium statistical thermodynamics.[14] Of course, by definition, the chemical potential of a crystal in complete equilibrium is uniform everywhere. But, if the *shape* of the solid does not conform to the equilibrium form, it must be the case that chemical potential gradients exist which (by some form of Fick's law) drive mass transport until morphological equilibrium is attained. To be more precise, consider a crystal in the shape of a parallelepiped (Fig. 1) and suppose that the Wulff plot[1,8] for this (fictitious) material is such that the crystal possesses only two inequivalent crystallographic facets with surface energies γ_1 and γ_2 (see the Appendix). According to Gibbs,[15] the average[16] chemical potential for particles just beneath the surface of these facets differs from that of particles deep in the (infinite) bulk by a correction which depends upon the finite size of the sample. For the geometry of Fig. 1 one has

$$\mu_1=\mu_c+f_1,\quad f_1=\frac{2\Omega\gamma_1}{l_1}+\frac{2\Omega\gamma_2}{l_2} \tag{1}$$

and

$$\mu_2=\mu_c+f_2,\quad f_2=\frac{4\Omega\gamma_1}{l_1}\ , \tag{2}$$

where μ_c is the chemical potential of the bulk and Ω is the volume of a particle. The gradient noted above exists

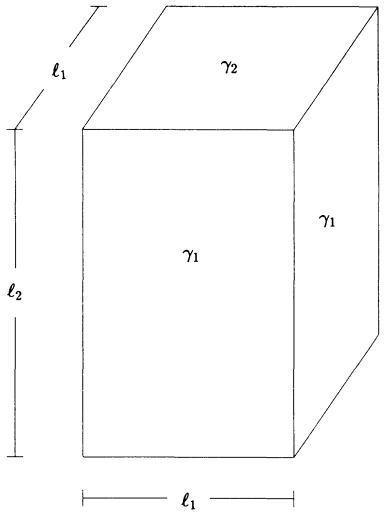

FIG. 1. The crystal shape discussed in the text. The Wulff plot of the fictitious material in question supports no facets beyond those depicted.

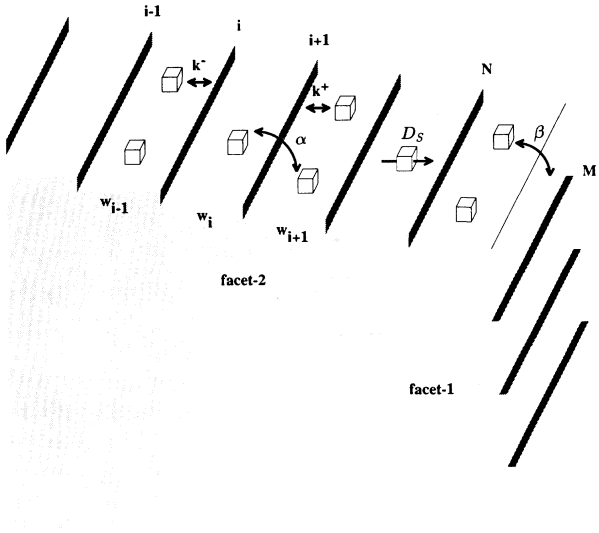

FIG. 2. An expanded view of a convex (exterior) corner of the parallelepiped shown in Fig. 1 which reveals the step structure of the facets. Although shown as straight, the step edges should be regarded as densely populated by kinks. The kinetic processes depicted are surface diffusion (D_S), exchange of atoms between terrace sites at an "up step" (k^+), exchange of atoms between terrace sites at a "down step" (k^-), exchange of adatoms between terraces on the *same* facet (α), and exchange of adatoms between terraces on *adjacent* facets (β).

because $\mu_1 \neq \mu_2$ unless the linear dimensions l_1 and l_2 attain their equilibrium values l_{1e} and l_{2e} defined by

$$\frac{\gamma_1}{l_{1e}} = \frac{\gamma_2}{l_{2e}} \ . \tag{3}$$

In that case, the common chemical potential of the system becomes, e.g.,

$$\mu = \mu_c + \frac{4\Omega\gamma_1}{l_{1e}} \tag{4}$$

which will be recognized as a Gibbs-Thomson formula.

Regarding the kinetics, we will in this paper suppose that mass transport occurs by surface diffusion exclusively rather than by bulk diffusion or evaporation and recondensation. According to Kern,[8] this is a reasonable assumption if one restricts attention to small (≤ 100 μm) crystallites. For definiteness, suppose that the relative magnitudes of (1) and (2) are such that a transfer of atoms occurs from sites just beneath the surface of the top facet to sites just beneath the surface of the side facet in Fig. 2. On each facet, these sites are to be identified with the so-called *kink* sites of a monatomic step.[17] The transfer process then is mediated by a number of distinct kinetic processes: (i) exchange of atoms between terrace sites and kink sites at a bounding "up step" (k^+); (ii) exchange of atoms between terrace sites and kink sites at a bounding "down step" (k^-); (iii) surface diffusion across a terrace (D_S); (iv) exchange of adatoms between terraces on the same facet (α); (v) exchange of adatoms between terraces on adjacent facets (β). The quantities in parentheses above denote overall Arrhenius-type rate constants associated with each of these processes.

In what follows, we do not confront this most general formulation of the equilibration problem right away. Rather, various kinetic processes (representing different levels of approximation) are introduced progressively. In that way, one gains a better appreciation not only of their relative importance but also of the mathematical formalism we employ. Direct comparisons with previous studies are facilitated as well. Accordingly, Sec. II both introduces our methodology and solves the problem analytically at three different levels of approximation for the three-dimensional geometry of Fig. 1. For reasons to appear below, we turn to a two-dimensional geometry in Sec. III and numerically study the complete kinetics of morphological equilibration. Section IV summarizes our results, discusses some limitations of our approach, and suggests a few directions for future research.

II. ANALYTIC RESULTS IN 3D

A. Edges

The simplest approximation one can imagine for the problem at hand completely ignores the terrace-step-kink structure of the free surfaces. Instead, one envisages a *homogeneous* transfer of mass by the "flow" of an infinitesimally thin (dl_2) layer of material from each of the top and bottom surfaces of Fig. 1 "over the edges" to form a uniform coating (dl_1) on each of the sidewall surfaces. Although all of the aforementioned atomistic processes are avoided, one nevertheless can associate an elementary rate Λ with this imagined process. Then, according to Keizer's formulation of the kinetics of nonequilibrium processes,[14] the time variation of the average number of particles just beneath each surface can be written as

$$\frac{dN_1}{dt}=\Lambda\frac{2l_1}{a}\left[\exp\left[\frac{\mu_2}{k_BT}\right]-\exp\left[\frac{\mu_1}{k_BT}\right]\right] \tag{5}$$

for each of the sidewalls (hereafter collectively denoted "facet-1") and

$$\frac{dN_2}{dt}=\Lambda\frac{4l_1}{a}\left[\exp\left[\frac{\mu_1}{k_BT}\right]-\exp\left[\frac{\mu_2}{k_BT}\right]\right] \tag{6}$$

for the top and bottom facets (hereafter collectively denoted "facet-2"). In these expressions, μ_1 and μ_2 are given by (1) and (2) and the perimeter factors $4l_1/a$ and $2l_1/a$ (a is the lattice constant) count the number of "reaction centers" for the transfer process. They differ because there is no mass transfer between equivalent side facets. Conservation of total mass is respected since

$$\frac{dN_2}{dt}+2\frac{dN_1}{dt}=0\ . \tag{7}$$

The time variation of the geometrical dimensions of the parallelepiped are obtained directly from (5) and (6) using the fact that

$$dN_1=\frac{l_1l_2\,dl_1}{2\Omega}\quad\text{and}\quad dN_2=\frac{l_1^2\,dl_2}{2\Omega}\ . \tag{8}$$

The factors of 2 arise because particles from each pair of parallel facets contribute to the change in one linear dimension. The Fick's-law character of the resulting equations of motion is seen most directly if we consider the limit where $f_1,f_2\ll k_BT$ so that the size-dependent part of the above exponentials can be linearized. The result is

$$\begin{aligned}\frac{dl_1}{dt}&=\frac{2\Omega\Lambda e^{\mu_c/k_BT}}{k_BT}\frac{2}{al_2}(f_2-f_1)\ ,\\ \frac{dl_2}{dt}&=\frac{2\Omega\Lambda e^{\mu_c/k_BT}}{k_BT}\frac{4}{al_1}(f_1-f_2)\ .\end{aligned} \tag{9}$$

Using (3) and the conservation of volume ($V=l_1^2l_2=l_{1e}^2l_{2e}$), these two can be written in the form

$$\begin{aligned}\frac{dl_1}{dt}&=-\frac{8\Omega^2\Lambda\gamma_2e^{\mu_c/k_BT}}{k_BTV^2a}l_1(l_1^3-l_{1e}^3)\ ,\\ \frac{dl_2}{dt}&=-\frac{16\Omega^2\Lambda\gamma_1e^{\mu_c/k_BT}}{k_BTVa}l_2^{-1/2}(l_2^{3/2}-l_{2e}^{3/2})\ .\end{aligned} \tag{10}$$

Although these equations are exactly solvable, the solution assumes a simple form only when the initial crystal dimensions (l_{1o},l_{2o}) are not far from their equilibrium values. In that case one finds

$$\begin{aligned}\frac{l_1-l_{1e}}{l_{1o}-l_{1e}}&=\exp\left[-\frac{24\Omega^2\Lambda\gamma_2e^{\mu_c/k_BT}}{k_BTal_{2e}^2l_{1e}}t\right]\ ,\\ \frac{l_2^{1/2}-l_{2e}^{1/2}}{l_{2o}^{1/2}-l_{2e}^{1/2}}&=\exp\left[-\frac{24\Omega^2\Lambda\gamma_1e^{\mu_c/k_BT}}{k_BTal_{1e}^2l_{2e}}t\right]\ .\end{aligned} \tag{11}$$

For future reference, please note carefully the dependence of the exponential decay constant on the equilibrium crystal dimensions.

B. Kinks and edges

A more realistic description of morphological equilibration is obtained if we take explicit account of the fact that mobile atoms adsorbed on terraces are the true agents of mass transport. These adatoms appear by detachment from kink sites on one facet, migrate to an adjacent facet, and then disappear by attachment to a kink site on the second facet. This is the picture adopted by Bermond and Venables[7] in their study of this problem. Note that neither the spatial distribution of kinks nor the mechanism of adatom migration is specified at this level of approximation.

To be quantitative, let n_1 and n_2 denote the areal density of adatoms on the two inequivalent facets and let Λ_1, Λ_2, Λ_{12}, and Λ_{21} denote, respectively, the elementary rate constants for adatom-kink kinetics on facet-1, adatom-kink kinetics on facet-2, adatom transfer from facet-1 to facet-2, and adatom transfer from facet-2 to facet-1. Again following Keizer,[14] we find[18] that

$$\begin{aligned}\frac{dn_1}{dt}=&\Lambda_1n_{k1}\left[\exp\left[\frac{\mu_1}{k_BT}\right]-\exp\left[\frac{\bar\mu_1}{k_BT}\right]\right]\\ &+\Lambda_{12}\frac{2}{al_2}\left[\exp\left[\frac{\bar\mu_2}{k_BT}\right]-\exp\left[\frac{\bar\mu_1}{k_BT}\right]\right]\end{aligned} \tag{12}$$

and

$$\begin{aligned}\frac{dn_2}{dt}=&\Lambda_2n_{k2}\left[\exp\left[\frac{\mu_2}{k_BT}\right]-\exp\left[\frac{\bar\mu_2}{k_BT}\right]\right]\\ &+\Lambda_{21}\frac{4}{al_1}\left[\exp\left[\frac{\bar\mu_1}{k_BT}\right]-\exp\left[\frac{\bar\mu_2}{k_BT}\right]\right]\ ,\end{aligned} \tag{13}$$

where n_{k1} and n_{k2} denote the *uniform* (and presumed constant) areal density of kinks on the two facets and $\bar\mu_1$ and $\bar\mu_2$ are the chemical potentials of mobile adatoms on the facets. The latter are given by the standard[19] expression

$$\bar\mu_i=-\varepsilon_i+k_BT\ln\left[\frac{n_i}{n_Q}\right]\ , \tag{14}$$

where ε_i is the magnitude of the binding energy of an adatom to a terrace site on the ith facet and n_Q is a temperature-dependent constant.[20]

To simplify the notation, we shall suppose henceforth that $\varepsilon_1=\varepsilon_2=\varepsilon$.[21] Then, making use of the fact that $\Lambda_{12}=\Lambda_{21}=\Lambda$,[22] we rewrite (12) and (13) as

$$\frac{dn_1}{dt}=-\bar k_1(n_1-n_{1e})-\frac{2\bar\beta}{al_2n_Q}(n_1-n_2)\ , \tag{15}$$

$$\frac{dn_2}{dt}=-\bar k_2(n_2-n_{2e})-\frac{4\bar\beta}{al_1n_Q}(n_2-n_1) \tag{16}$$

in terms of lumped rate coefficients

$$\bar{k}_1=\Lambda_1\frac{n_{k1}}{n_Q}e^{-\varepsilon/k_BT},$$
$$\bar{k}_2=\Lambda_2\frac{n_{k2}}{n_Q}e^{-\varepsilon/k_BT}, \quad (17)$$
$$\bar{\beta}=\Lambda e^{-\varepsilon/k_BT},$$

and equilibrium adatom concentrations

$$n_{1e}=n_Q\exp\left[\frac{\mu_c+\varepsilon+f_1}{k_BT}\right],$$
$$n_{2e}=n_Q\exp\left[\frac{\mu_c+\varepsilon+f_2}{k_BT}\right]. \quad (18)$$

It is crucial to observe that n_{1e} and n_{2e} depend explicitly on the facet sizes through the factors f_1 and f_2 [cf. (1) and (2)]. In fact, it is precisely this factor in the first term of (15) and (16) that induces each facet to either grow or etch in the direction perpendicular to itself. The second term merely transfers mobile species from one facet to the other without directly affecting the solid. Accordingly, the crystal dimensions evolve as

$$\frac{1}{2\Omega}\frac{dl_1}{dt}=\bar{k}_1(n_1-n_{1e}), \quad \frac{1}{2\Omega}\frac{dl_2}{dt}=\bar{k}_2(n_2-n_{2e}). \quad (19)$$

The complete kinetics of equilibration is obtained from (19) once (15) and (16) have been solved. Although this generally requires a numerical approach, a steady-state solution can be obtained analytically in certain limits. In particular, one verifies readily that if $\dot{n}_1=\dot{n}_2=0$,

$$\frac{dl_1}{dt}=\frac{2\Omega(n_{2e}-n_{1e})}{\tau_1}, \quad (20)$$
$$\frac{dl_2}{dt}=-\frac{4\Omega(n_{2e}-n_{1e})}{\tau_2}, \quad (21)$$

where

$$\tau_1=\frac{1}{\bar{k}_1}+\frac{2}{\bar{k}_2}\frac{l_2}{l_1}+\frac{an_Ql_2}{2\bar{\beta}},$$
$$\tau_2=\frac{1}{\bar{k}_1}\frac{l_1}{l_2}+\frac{2}{\bar{k}_2}+\frac{an_Ql_l}{2\bar{\beta}}. \quad (22)$$

Linearizing the size-dependent part of the exponentials in (18) and proceeding as in the passage from (9) to (10), we obtain

$$\frac{dl_1}{dt}=-\frac{4n_Q\Omega^2\gamma_2}{k_BTVl_1\tau_1}e^{(\mu_c+\varepsilon)/k_BT}(l_1^3-l_{1e}^3), \quad (23)$$
$$\frac{dl_2}{dt}=-\frac{8n_Q\Omega^2\gamma_1}{k_BT\sqrt{V}l_2\tau_2}e^{(\mu_c+\varepsilon)/k_BT}(l_2^{3/2}-l_{2e}^{3/2}). \quad (24)$$

Again, a particularly simple exact solution is obtained if the initial crystal shape does not differ too much from the equilibrium form. In that case, one finds

$$l_1-l_{1e}=(l_{1o}-l_{1e})\exp\left[-\frac{6\gamma_2\sigma}{l_{1e}l_{2e}}\frac{t}{\tau_{1e}}\right], \quad (25)$$

$$l_2^{1/2}-l_{2e}^{1/2}=(l_{2o}^{1/2}-l_{2e}^{1/2})\exp\left[-\frac{6\gamma_1\sigma}{l_{1e}l_{2e}}\frac{t}{\tau_{2e}}\right], \quad (26)$$

where

$$\sigma=\frac{2n_Q\Omega^2}{k_BT}e^{(\mu_c+\varepsilon)/k_BT} \quad (27)$$

and τ_{1e} and τ_{2e} denote the time constants (22) evaluated at the equilibrium crystal dimensions.

It is satisfying to note that if interfacet particle transfer is rate limiting, i.e., $\bar{\beta}\ll\bar{k}_1,\bar{k}_2$, the time constants simplify such that (25) and (26) reproduce (11) *exactly*. On the other hand, different dependences for the facet size decay rates on the equilibrium crystal dimensions emerge if, instead, the kinetics of adatom attachment and detachment to and from kinks on either of the inequivalent facets is rate limiting. For example, l_1 approaches its equilibrium value at a rate which depends on the factor $l_{1e}l_{2e}$ (l_{2e}^2) for the case of slow kinetics on facet-1 (facet-2). Similarly, l_2 approaches its equilibrium value at a rate which depends on the factor l_{1e}^2 ($l_{1e}l_{2e}$) for the case of slow kinetics on facet-1 (facet-2). Although these results agree with those of Ref. 7 in the corresponding limit, we have reservations[23] concerning their results in the general case.

C. Steps and kinks and edges

This section presents our most complete account of the kinetic processes that contribute to morphological equilibration. Compared to the discussion above, we (i) correct the assumption of a uniform distribution of kinks by properly associating them with monatomic steps, and (ii) explicitly treat the transport of adatoms by surface diffusion. In such a treatment, the steps acquire a dynamics of their own (they advance or recede across a facet as adatoms attach or detach from them). To simplify this aspect of the problem, we shall assume that the density of kink sites *along* each step is sufficiently great that every point along the step may be regarded as a source or sink for adatoms. For the geometry of Fig. 2, this renders the problem one dimensional.[24] Moreover, once step dynamics are admitted into the problem, it is necessary to take account of the well-established fact that adjacent steps generally *repel* one another due to elastic[25] and/or entropic effects.[26] This phenomenon is included most conveniently[12,13] as an additive correction to the chemical potential for atoms just at the step. Thus, e.g., for a step labeled i on the "top" facet-2 of Fig. 2 one writes in place of (2)

$$\mu_2^i=\mu_c+\frac{4\Omega\gamma_1}{l_1}+\mu_2^i(s), \quad \mu_2^i(s)=\Gamma_2\left[\frac{1}{w_i^3}-\frac{1}{w_{i-1}^3}\right], \quad (28)$$

where Γ_2 is a constant characteristic of facet-2 and w_i is the width of the ith terrace.[27] In principle, the surface energy γ_1 in (28) should be renormalized to account for the presence of steps on the facet. The correction, however, is proportional to the linear step *density* (see, e.g., Ref. 11 and the Appendix) which must nevertheless remain small

to guarantee the validity of our model, which assumes that each facet is macroscopically flat. Finally, of course, it is necessary to verify that the presence of step-step interactions does not alter the equilibrium crystal shape from that presumed above. A demonstration that this is indeed the case (for a 2D crystal) may be found in the Appendix.

As in the preceding section, we focus on the concentration of mobile adatoms. However, since we now propose to take account of surface diffusion, this quantity varies in space as well as in time. The appropriate generalization of formulas such as (12) and (13) is a so-called reaction-diffusion equation of the form

$$\frac{\partial n}{\partial t}=D_S\frac{\partial^2 n}{\partial x^2}+\sum_k R_k\delta(x-x_k)\ , \tag{29}$$

where D_S is the surface diffusion constant and the R_k are expressions like those on the right-hand sides of (12) and (13). The latter describe the rates of kinetic processes that are now *localized* at step and edges located at absolute positions x_k.

Although (29) (and an initial condition) completely specifies the problem, this equation is difficult to deal with directly due to the presence of the δ functions. On the other hand, it is readily established[28] that (29) is completely equivalent to an *ordinary* diffusion equation

$$\frac{\partial n}{\partial t}=D_S\frac{\partial^2 n}{\partial x^2} \tag{30}$$

valid on each terrace supplemented by two "jump" boundary conditions obtained by integrating (29) over an interval $(x_k-\delta,\ x_k+\delta)$ once for each of the two steps that bounds that terrace.

To be more specific, consider as an example an arbitrary step i somewhere on facet-2 of Fig. 2 and suppose that the only kinetic processes operative are the attachment and detachment of atoms to and from the step from both bounding terraces. In that case, the integration noted above yields (in the limit $\delta\to 0$)

$$D_S\left[\left.\frac{\partial n_2}{\partial x}\right|_{x_i^+}-\left.\frac{\partial n_2}{\partial x}\right|_{x_i^-}\right]=\frac{\Lambda_2^+}{a}\left[\exp\left[\frac{\bar{\mu}_2(x_i^+)}{k_BT}\right]-\exp\left[\frac{\mu_2^i}{k_BT}\right]\right]+\frac{\Lambda_2^-}{a}\left[\exp\left[\frac{\bar{\mu}_2(x_i^-)}{k_BT}\right]-\exp\left[\frac{\mu_2^i}{k_BT}\right]\right]\ , \tag{31}$$

where Λ_2^+ (Λ_2^-) denotes the elementary rate for adatom attachment and detachment to and from a step on facet-2 from a lower (upper) bounding terrace.[29] Although not obvious from the present discussion, it can be shown using the methods of Ref. 14 that (31) actually breaks into *two* equations—each confined to quantities evaluated on one side of the step. Consequently, expressing the chemical potentials in terms of adatom concentrations using (14) and (18), the full boundary conditions for (30) associated with each step can be written

$$\begin{aligned}D_S\left.\frac{\partial n_i}{\partial x}\right|_{x_i^+}&=k_2^+[n_i(x_i^+)-n_{2e}e^{\mu_2^i(s)/k_BT}]\\&\quad+\alpha[n_i(x_i^+)-n_{i-1}(x_i^-)]\ ,\\-D_S\left.\frac{\partial n_{i-1}}{\partial x}\right|_{x_i^-}&=k_2^-[n_{i-1}(x_i^-)-n_{2e}e^{\mu_2^i(s)/k_BT}]\\&\quad+\alpha[n_{i-1}(x_i^-)-n_i(x_i^+)]\ ,\end{aligned} \tag{32}$$

where we have included the effect of adatoms hopping directly over the step with the terms proportional to the kinetic coefficient α. In addition, we have defined the lumped kinetic coefficients

$$k_2^+=\frac{\Lambda_2^+}{an_Q}e^{-\varepsilon/k_BT}\ ,\quad k_2^-=\frac{\Lambda_2^-}{an_Q}e^{-\varepsilon/k_BT}\ , \tag{33}$$

and introduced the notation n_i to denote the adatom concentration on the ith terrace (all such quantities are understood here to belong to facet-2).

To compete the roster of kinetic processes listed in the Introduction, we need only write boundary conditions analogous to (32) for an edge where two inequivalent facets meet. Denoting the position of one such edge by x_0, the appropriate equations are

$$D_S\left.\frac{\partial n_M}{\partial x}\right|_{x_0^+}=\beta n_M(x_0^+)-\beta n_N(x_0^-)=-D_S\left.\frac{\partial n_N}{\partial x}\right|_{x_0^-}\ , \tag{34}$$

where the integers M and N, respectively, identify the terraces of facet-1 and facet-2, which meet at x_0. The inter-facet transfer coefficient is defined by

$$\beta=\frac{\Lambda}{an_Q}e^{-\varepsilon/k_BT}\ . \tag{35}$$

Consistent with our earlier choice of $\varepsilon_1=\varepsilon_2=\varepsilon$, the surface diffusion constants of the two facets are taken equal.

We now have all the ingredients required to complete our description of morphological equilibration. However, the reader will have noticed that the *origin* of the steps required to effect mass transport has so far been left unstated. To correct this omission, return to the three-dimensional geometry of Fig. 1. Long ago, Gibbs[30] noted that, in equilibrium, the very loosely bound atoms at the edges of such a crystal often will be absent due to thermal fluctuations. In a nonstatistical treatment such as ours, this implies that we may presume the presence of a single monatomic step along every edge. To exploit this fact, we analyze a simple problem wherein no more than one step is present (on each facet) during the equilibration process. Although somewhat artificial, this model has the virtue that it can be solved analytically so that direct comparison can be made with our own previous results (and those of others).

The crystal morphology during mass transfer always

appears as shown in Fig. 3. The step which forms the perimeter of the single (shrinking), square, monatomic island on facet-2 originated as the equilibrium step noted above. The single (growing) island on facet-1 is presumed to have formed instantaneously and symmetrically to provide a sink for adatoms diffusing from facet-2. Both processes are imagined to repeat when required. We further suppose that adatoms diffuse along straight lines between escape and capture from steps. In that case, the steady-state solution to (30) takes the form

$$n_i(x)=a_i+b_i x, \quad x_i<x<x_{1+i} \tag{36}$$

on every facet. We ignore, for the moment, the fact that this approximation is invalid whenever either island is small compared to the corresponding facet size.

Since multiple steps never occur, step-step interactions (28) are absent. Moreover, by symmetry, the adatom population is uniform ($b_i\equiv 0$) on those terraces which form the tops of the islands. The boundary conditions (32) and (34) then permit calculation of the coefficients in (36) for the single remaining terrace on each facet (labeled by widths w_1 and s_1 in Fig. 3). For the problem at hand, it turns out that the corresponding coefficients are *equal* on the two terraces for the second term in (36). The common value is

$$b=\frac{a(n_{2e}-n_{1e})}{\tau D_S}\ , \tag{37}$$

where

$$\tau=a\left[\frac{\kappa_1^-}{\mathcal{K}_1}+\frac{\kappa_2^-}{\mathcal{K}_2}+\frac{1}{\beta}+\frac{w_1+s_1}{D_S}\right]=\frac{a}{D_S}(L_{\mathcal{K}}+w_1+s_1) \tag{38}$$

with

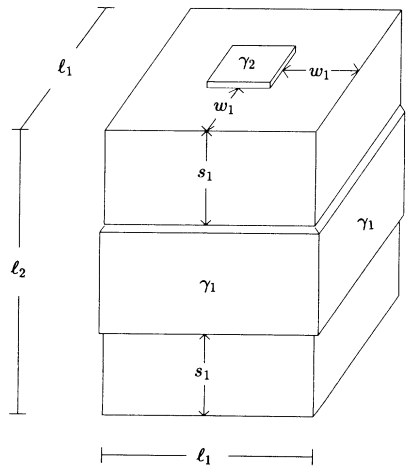

FIG. 3. Same as Fig. 1 except that there is a single island (of monolayer height) on each facet. During equilibration, the square island on each face of facet-2 shrinks and the rectangular island on each face of facet-1 grows.

$$\kappa_1^{\pm}=k_1^{\pm}+\alpha, \quad \kappa_2^{\pm}=k_2^{\pm}+\alpha, \quad \mathcal{K}_i=\kappa_i^+\kappa_i^- -\alpha^2, \quad i=1,2\ . \tag{39}$$

Now, by mass conservation,[13,31] the velocity of any step in Fig. 2 is

$$\frac{dx_i}{dt}=a^2D_S\left[\left.\frac{dn_i}{dx}\right|_{x_i^+}-\left.\frac{dn_{i-1}}{dx}\right|_{x_i^-}\right] \tag{40}$$

so that

$$\frac{dw_1}{dt}=-a^2D_S b, \quad \frac{ds_1}{dt}=a^2D_S\left[1-\frac{2w_1}{l_1}\right]b\ . \tag{41}$$

The factor in parentheses arises because the mass transferred from the islands of facet-2 in Fig. 3 is presumed to distribute uniformly along the steps of facet-1. Observe, however, that to the extent that this factor may be neglected,

$$\frac{d}{dt}(w_1+s_1)=0 \tag{42}$$

and τ may be replaced by the constant τ_0 obtained from (38) by replacing w_1 and s_1 with, e.g., their initial values. The terrace widths themselves evolve as *linear* functions of time.

To facilitate comparison with our previous results, we make a continuum approximation to (41) by reassigning the mass lost by the islands of facet-2 to a thin layer removed uniformly from the area of that facet. The mass gained by facet-1 is treated similarly. The explicit relation is

$$\frac{dl_1}{dt}=\frac{4a}{l_2}\frac{ds_1}{dt}, \quad \frac{dl_2}{dt}=-\frac{8a}{l_1}\frac{ds_1}{dt}\ . \tag{43}$$

From these, one readily obtains (in the limit $2w_1/l_1\ll 1$)

$$\frac{dl_1}{dt}=-\frac{8\sigma\gamma_2 a}{l_1 l_2 V\tau_0}(l_1^3-l_{1e}^3)\ . \tag{44}$$

A similar equation holds for l_2. If finally, as a simplification, we suppose that $k_1^{\pm}=k_1$ and $k_2^{\pm}=k_2$ so that

$$\tau_0=a\left[\frac{1}{k_1\left[1+\frac{1}{1+k_1/\alpha}\right]}+\frac{1}{k_2\left[1+\frac{1}{1+k_2/\alpha}\right]}+\frac{1}{\beta}+\frac{w_{1o}+s_{1o}}{D_S}\right], \tag{45}$$

the late stage evolution of $l_1(t)$ obeys

$$l_1-l_{1e}=(l_{1o}-l_{1e})\exp\left[-\frac{12\gamma_2\sigma}{l_{1e}l_{2e}}\frac{a}{l_{2e}}\frac{t}{\tau_o}\right]\ . \tag{46}$$

To appreciate this result, suppose first that surface diffusion is very *fast* ($D_S\to\infty$) and that the direct transfer of particles between terraces belonging to the same facet is very *slow* ($\alpha\to 0$). In that case, it is easy to check from

(45) that in each of the three limits discussed at the end of Sec. II B, i.e., β or k_1 or k_2 rate limiting, (46) reduces to (25) exactly. Or, more precisely [noting the difference in the definitions of $k_i^{\pm}$ and $\bar{k}_i$ in (33) and (17), respectively], this equivalence occurs *if* the kink densities in (17) are chosen as

$$n_{k1}=\frac{2l_{1e}/a}{l_{1e}l_{2e}}, \quad n_{k2}=\frac{4l_{1e}/a}{l_{1e}^2} . \tag{47}$$

These values are precisely those required to distribute *uniformly* over each facet the total number of kinks present on that facet in Fig. 3 at the very beginning of the equilibration process. In the case when $\alpha\to\infty$, i.e., terrace-to-terrace transfer is the fastest of all processes, one sees that the rates of kink-mediated equilibration are exactly doubled.

A noteworthy result is found from the foregoing if surface diffusion is rate limiting. In that case, the *overall* exponential time constant in (46) is proportional to the geometric factor $l_{1e}l_{2e}^2(w_{1o}+s_{1o})$. This may be compared to the analyses of Bermond and Venables[7] and Kern,[8] both of whom find a time constant that varies as $l_{1e}^2l_{2e}^2$. In fact, it may be argued that these agree given that both of these authors essentially choose the rate coefficient we call Λ proportional to D_S. On the other hand, we have had to make some rather drastic approximations in order to make these comparisons possible. For example, the quantity $w_{1o}+s_{1o}$ is not truly a constant but changes each time a new step is created. This is significant because the full richness of our approach becomes evident only if we retain the discrete nature of the steps throughout the entire time evolution of the facets. Unfortunately, to do so we must abandon the case of a three-dimensional crystal treated so far in order to guarantee that none of our results are tainted by the very approximate treatment of the diffusion problem employed above. As it happens, we are able to treat the case of a two-dimensional crystal essentially exactly. In our view, the interesting results that emerge more than compensate the attendant retreat from direct experimental relevance.

III. NUMERICAL RESULTS IN 2D

Only very minor changes in the formalism of the preceding section are required for a crystal comprised of only the front face (area $A=l_1l_2$) of Fig. 1. Thus, while (1) and (2) are replaced by

$$\mu_1=\mu_c+\frac{2\Omega\gamma_2}{l_2}, \quad \mu_2=\mu_c+\frac{2\Omega\gamma_1}{l_1} , \tag{48}$$

the entire discussion of the one-dimensional diffusion equation and its boundary conditions carries over without change. It is instructive to begin with a reexamination of the single-step model introduced just above. In two dimensions, one readily verifies that

$$\frac{dw_1}{dt}=-a^2D_Sb, \quad \frac{ds_1}{dt}=a^2D_Sb , \tag{49}$$

without approximation so that (42) is exact as well. The expression (37) for b is unchanged except for the redefinition of f_1 and f_2 in (18) implied by (48). In our numerical implementation of (49), the island on facet-2 shrinks while the one on facet-1 grows. At the moment the former disappears, we create a step at each edge of facet-2 to insure that there is always exactly one island there. Similarly, at the moment the island on facet-1 grows to cover the entire face, we create a new island atop it at the center. A discrete change in l_1 or l_2 (by 2a) is recorded only at these moments.

The time histories $l_1(t)$ and $l_2(t)$ obtained from the foregoing are compared most usefully to those obtained by integrating the corresponding continuum equations of motion:

$$\frac{dl_1}{dt}=\frac{4a}{l_2}\frac{ds_1}{dt}=-\frac{4\sigma\gamma_2a}{\tau_0A^2}(l_1^2-l_{1e}^2) , \tag{50}$$

$$\frac{dl_2}{dt}=-\frac{4a}{l_1}\frac{ds_1}{dt}=-\frac{4\sigma\gamma_1a}{\tau_0A^2}(l_2^2-l_{2e}^2) . \tag{51}$$

Typical results are shown in Fig. 4 for three choices of the lumped kinetic parameter $L_{\mathcal{K}}$. As can be seen from (38), this quantity is a length which may be thought of as the distance an adatom can diffuse in the time required for the slowest of the remaining kinetic processes to occur. Here (and below) we choose $\gamma_1=\gamma_2$ so that the equilibrium crystal shape is a square (see the Appendix). The solid and dashed lines, respectively, denote the exact and continuum kinetics. For the latter, it is necessary to assign a value to the quantity $w_{1o}+s_{1o}$ in (45). For reasons to appear momentarily, we have chosen the value $l_e/3$. Observe that for large values of $L_{\mathcal{K}}$ (compared to the crystal dimensions) the approximate solution slightly overestimates the equilibration time while for small values of $L_{\mathcal{K}}$ it is underestimated.

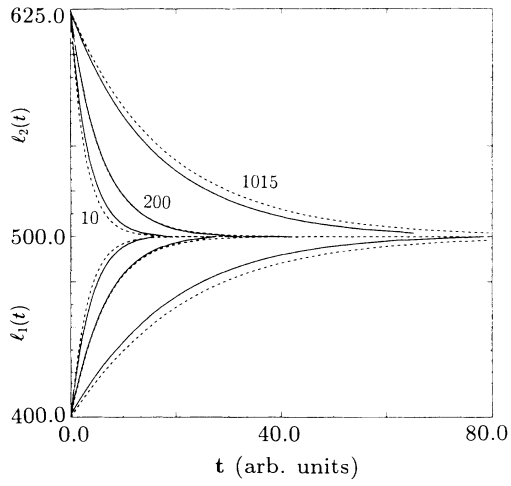

FIG. 4. The variation of facet lengths as a function of time (equilibration curves) for the single-step model. The solid lines correspond to the exact, discrete step kinetics [Eq. (49)]. The dashed lines correspond to the solution of the approximate continuum equations (50) and (51). The number on each curve is the numerical value of the parameter $L_{\mathcal{K}}$.

The specific choice noted above for evaluation of the continuum model was made because, if $w_{1o}+s_{1o}$ is set equal to $(l_1+l_2)/6$, (50) and (51) exactly coincide (when surface diffusion is rate limiting) with equations of motion derived for this problem by Yu and Hackney.[9] In that work, the chemical potential is presumed to vary across a facet in a manner determined by (i) a well-known[11] relation between the Laplacian of the chemical potential and the *normal* velocity of a surface element and (ii) the requirement that the normal velocity be constant across the entire facet. Although the very fact of facet growth by discrete step propagation clearly reveals the approximate nature of these assumptions, their approach provides additional insight into the nature of the continuum limit of single-step kinetics.

Of course, the single-step model artificially precludes the possibility of multiple-step generation on one (or both) facets. In reality,[32] both step formation at a crystal edge and island nucleation on a crystal terrace are activated processes whose probability depends upon the concentration of adatoms at the point in question. Relative to the equilibrium adatom density, undersaturation promotes the former while supersaturation stimulates the latter. If, say, interfacet adatom transfer is very fast, it is reasonable to expect a rapid depletion of mobile species in the immediate neighborhood of an edge of facet-2. Creation of a new step (or steps) at that point provides a source of adatoms which tends to bring the population back to its equilibrium value. A similar scenario of island nucleation events tends to relieve a surfeit of adatoms on the terraces of facet-1.

As it happens, the computations required to evaluate the adatom concentrations needed above are precisely those required to calculate the step kinetics. Namely, solution of the diffusion equation (30) (in steady state) subject to reaction-type boundary conditions at the steps (32) and edges (34). The (symmetric) geometry under consideration is shown in Fig. 5. If, for the sake of clarity, we use the variable y to denote the spatial position on facet-1, the appropriate generalization of (36) is

$$n_i(x)=a_i+b_i x, \quad 0\le i\le N, \quad x_i<x<x_{i+1} \tag{52}$$

for the adatom concentration on the terraces of facet-2 and

$$n_j(y)=c_j+d_j y, \quad 0\le j\le M, \quad y_{j+1}<y<y_j \tag{53}$$

for the terraces of facet-1. Again, by symmetry, $b_0=d_0=0$ on the topmost terraces. From (40), the terrace width velocities can be written

$$\begin{aligned}
&\dot{w}_1=a^2D_S(b_2-2b_1)\ ,\\
&\dot{w}_i=a^2D_S(b_{i+1}-2b_i+b_{i-1})\ , \quad 2\le i\le N-1\ ,\\
&\dot{w}_N=a^2D_S(b_{N-1}-b_N)
\end{aligned} \tag{54}$$

on facet-2 and

$$\begin{aligned}
&\dot{s}_1=-a^2D_S(d_2-2d_1)\ ,\\
&\dot{s}_j=-a^2D_S(d_{j+1}-2d_j+d_{j-1}), \quad 2\le j\le M-1\ ,\\
&\dot{s}_M=-a^2D_S(d_{M-1}-d_M)
\end{aligned} \tag{55}$$

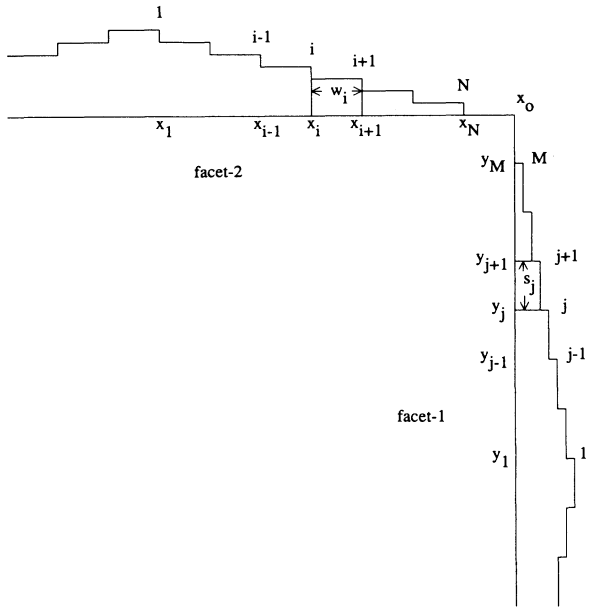

FIG. 5. Side view of Fig. 2 in two dimensions.

on facet-1. The b's and d's are determined (from the boundary conditions) by solution of the coupled linear equations:

$$\begin{aligned}
&b_i\left[\frac{D_S}{\mathcal{K}_2}(\kappa_2^+ +\kappa_2^-)+w_i\right]-\frac{D_S\alpha}{\mathcal{K}_2}(b_{i+1}+b_{i-1})\\
&\qquad=n_{2e}\left[\exp\left[\frac{\mu_2^i(s)}{k_BT}\right]-\exp\left[\frac{\mu_2^{i+1}(s)}{k_BT}\right]\right],
\end{aligned} \tag{56}$$

$$\begin{aligned}
&d_j\left[\frac{D_S}{\mathcal{K}_1}(\kappa_1^+ +\kappa_1^-)+s_j\right]-\frac{D_S\alpha}{\mathcal{K}_1}(d_{j+1}+d_{j-1})\\
&\qquad=n_{1e}\left[\exp\left[\frac{\mu_1^{j+1}(s)}{k_BT}\right]-\exp\left[\frac{\mu_1^{j}(s)}{k_BT}\right]\right],
\end{aligned} \tag{57}$$

and

$$\begin{aligned}
b_N=\frac{a}{\tau'}\Bigg\{&\frac{\alpha}{\mathcal{K}_2}b_{N-1}+\frac{\alpha}{\mathcal{K}_1}d_{M-1}\\
&+D_S^{-1}\left[n_{1e}\exp\left[\frac{\mu_1^M(s)}{k_BT}\right]\right.\\
&\left.\left.-n_{2e}\exp\left[\frac{\mu_2^N(s)}{k_BT}\right]\right]\right\}\\
=d_M\ ,&
\end{aligned} \tag{58}$$

where

$$\tau'=\frac{a}{D_S}(L_{\mathcal{K}}+w_N+s_M) \tag{59}$$

and $L_{\mathcal{K}}$ is as defined in (38).

The boundary conditions also determine all the a's and c's in (52) and (53), but we will need only two of them to compute the rates of step creation and island nucleation.

In particular, at the point x_0 on terrace N of facet-2,

$$n(x_0)=a_N+b_N x_0=\lambda_2 n_{2e} , \tag{60}$$

where

$$\lambda_2=\frac{1}{n_{2e}}\left[b_N\left[\frac{\kappa_2^- D_S}{\mathcal{K}_2}+w_N\right]-\frac{\beta D_S}{\mathcal{K}_2}b_{N-1}\right] +\exp\left[\frac{\mu_2^N(s)}{k_B T}\right] , \tag{61}$$

and at the center of the topmost terrace of facet-1,

$$n(y)=c_0=\lambda_1 n_{1e} , \tag{62}$$

where

$$\lambda_1=-\frac{\alpha D_S}{n_{1e}\mathcal{K}_1}d_1+\exp\left[\frac{\mu_1^1(s)}{k_B T}\right] . \tag{63}$$

So defined, the quantities λ_1 and λ_2 measure the relevant supersaturation and undersaturation. We have verified (analytically for the single-step case and numerically otherwise) that $\lambda_1 \geq 1$ and $0<\lambda_2 \leq 1$ as expected.

The number of steps present on any facet at a given time depends on all the kinetic coefficients, the strength of the step-step repulsion, and the size of the crystal. Nevertheless, to develop some feeling for the factors which promote step proliferation, it is useful to consider the form taken by (61) for the case of a single step on each facet with $\alpha=0$:

$$\lambda_2=\left[\frac{n_{1e}}{n_{2e}}-1\right]\left[1+\frac{s_1+D_S(1/k_1+1/\beta)}{\omega_1+D_S/k_2}\right]^{-1} . \tag{64}$$

From this one sees, for example, that small values of s_1 increase the relative undersaturation at the edge of the crystal and hence increases the probability for creation of a new step there. In other words, the rate of step creation on facet-2 increases when a layer on facet-1 is about to complete. Our numerical results confirm this prediction—even when many steps are present. Note also that when $L_{\mathcal{K}}$ is large the quantity in the second set of large parentheses in (64) approaches 2 and the undersaturation depends only on the crystal dimensions (through n_{1e} and n_{2e}).

Of course, the precise magnitudes of undersaturation and supersaturation required to trigger the activated processes of interest depend, e.g., on temperature. Consequently, we use the parameters λ_1^* and λ_2^* to control the nucleation process. That is, during the evolution of the system, a new step is created at the edge of facet-2 whenever the computed value of λ_2 falls below λ_2^*. Similarly, a new island is nucleated at the center of facet-1 whenever the computed value of λ_1 exceeds λ_1^*. Our model evidently contains many independent parameters. As it happens, the calculated value of λ_1 from (63) is always very close to 1 so that, unless λ_1^* is nearly unity, very few steps are generated on facet-1. Conversely, λ_2 from (61) depends strongly on the choice of parameters so there is much more dynamic range for λ_2^*. In what follows, we limit ourselves to one particular choice of these quantities which permits modest step generation on facet-2.

As for the case of the single step, it is convenient to organize the results according to the magnitude of the parameter $L_{\mathcal{K}}$. When $L_{\mathcal{K}}$ is large, each of k_1, β, and k_2 can be individually rate limiting. This is illustrated in Fig. 6(a). The first two cases are seen to be identical to one another and to the previous smooth single-step results. By contrast, when atom detachment from steps is difficult on facet-2 (k_2 small), equilibration occurs by a two-step process: a brief period of very large morphological change followed by a long interval of slow approach to the final equilibrium crystal dimensions. The same gen-

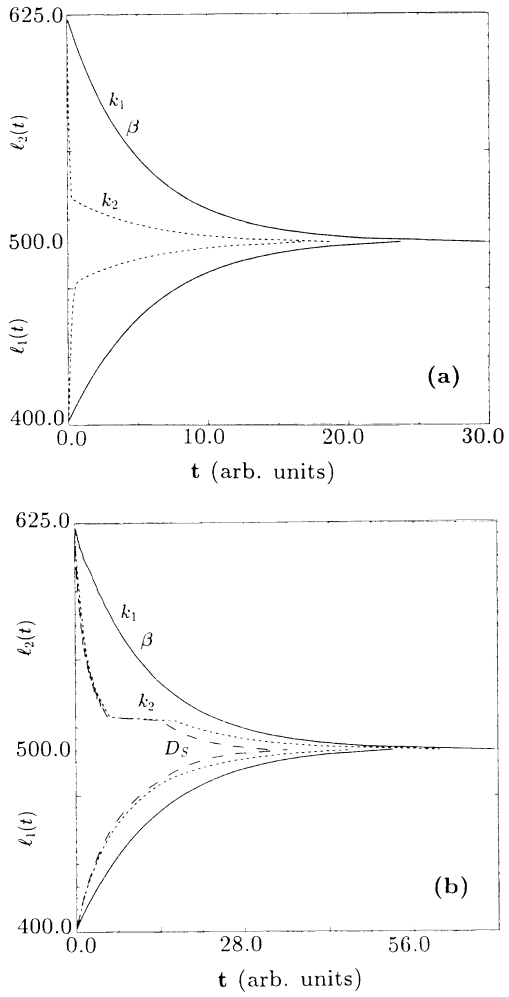

FIG. 6. (a) Equilibration curves when either k_1, β (same solid line for both), or k_2 (dashed line) is rate limiting for a (fixed) value of the parameter $L_{\mathcal{K}}$ large compared to the crystal dimensions. A large common value has been assigned to all other kinetic parameters; (b) Same as (a) except that the value of $L_{\mathcal{K}}$ is chosen comparable to the crystal dimensions for the cases when either k_1, β (same solid line for both), or k_2 (short-dashed lines) is rate limiting. The curve labeled D_S corresponds to $L_{\mathcal{K}}$ chosen very small compared to the crystal dimensions. For the latter, the time of equilibration is scaled by $1/D_S$ to facilitate comparison with the other curves.

eral behavior for these three cases is found when $L_{\mathcal{H}}$ is comparable to the crystal size [Fig. 6(b)] except that the k_2-limited equilibration curve now contains an additional period of evolution at intermediate times where one of the crystal dimensions changes very little. When $L_{\mathcal{H}} \ll l_1, l_2$, surface diffusion controls morphological evolution and the corresponding equilibration curve [labeled D_S in Fig. 6(b)] also exhibits three distinct regions of behavior.

All of the foregoing are best understood by direct inspection of the crystal morphologies as a function of time. Figure 7 illustrates the common behavior when either k_1 (step attachment on facet-1) or β (interfacet transfer) is rate limiting. Note that very few steps are generated during equilibration. This is so because the first of these tends to build up an adatom concentration on terrace s_M while the second tends to build up an adatom concentration on terrace w_N. In either case, the concentration of adatoms near the edge infrequently drops to the point where $\lambda_2 < \lambda_2^*$ and there is little step generation.

If neither interfacet transfer nor facet-1 step kinetics is rate limiting, equilibration always begins with a period of very rapid step proliferation. This is so because, in that case, either surface diffusion or atom detachment from steps on facet-2 limits the supply of free adatoms. Efficient mass transfer can occur only by the creation of many steps. This circumstance results in both a rapid change in the morphology of the crystal (Fig. 6) and in the creation of a step bunch on facet-2 (Fig. 8). Eventually, step repulsion becomes important and the crystal seeks to eliminate the bunch. This takes place by cooperative transfer of mass down the steps in a manner identical to that discussed by us in a previous paper.[13] Specifically, all terrace widths steadily increase in time except the one at the top of the bunch. This topmost terrace decreases in width until the steps which bound it collide and annihilate. The process repeats until all the mass in the bunch has been transferred. At the conclusion of this period, only one step remains on each facet and single-step dynamics determines the subsequent evolution.

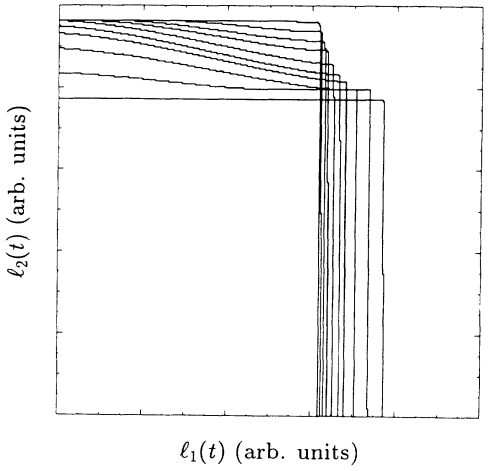

FIG. 8. Same as Fig. 7 for equilibration corresponding to either of the dashed curves in Fig. 6(b).

The presence or absence of the flat, intermediate region of evolution which distinguishes Fig. 6(a) from Fig. 6(b) is controlled entirely by the rate at which the foregoing cooperative process occurs. When $L_{\mathcal{H}} = D_S/k_2$ is large, the bunch is eliminated very rapidly [essentially instantaneously on the scale of Fig. 6(a)]. Conversely, when $L_{\mathcal{H}}$ is small, diffusing adatoms do not travel very far in the time between atomic detachments from steps and mass transfer down the step bunch is sluggish. The crystal dimension l_2 remains fixed as the bunch slowly dissolves. It is useful to recall here that, even in the presence of a bunch, facet-2 is macroscopically flat so l_2 is measured at the edge of facet-2 rather than at the top of the bunch (at the center of the facet).

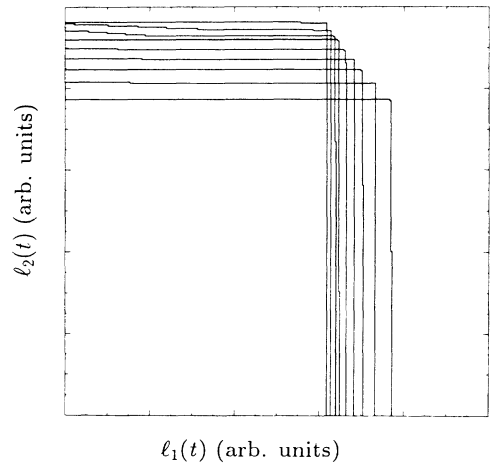

FIG. 7. The shape of one quarter of the crystal during equilibration corresponding to the solid curves in Fig. 6. The profiles correspond to *randomly* selected times of step creation or annihilation on either facet. By symmetry, the remaining quarters of the crystal evolve identically.

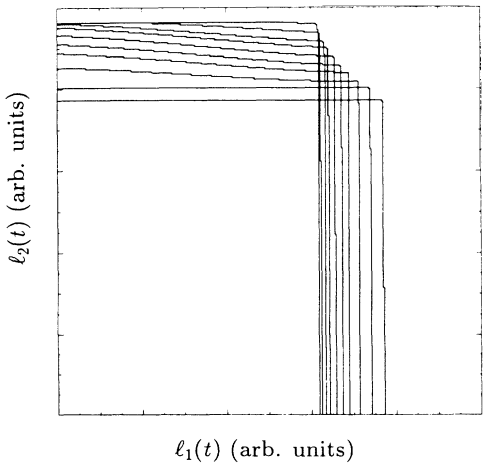

FIG. 9. Similar to Fig. 8 except that the strength of step-step repulsion is five times stronger.

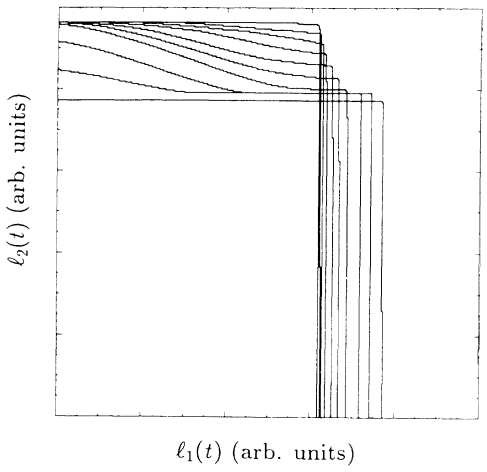

FIG. 10. Similar to Fig. 8 except that the strength of step-step repulsion is ten times weaker.

The number and distribution of steps in the foregoing scenario depends strongly on the magnitude of the repulsion between the steps. Figures 9 and 10 are comparable to Fig. 8 (k_2 rate limiting) except that the step repulsion [controlled by the parameter Γ in (28)] is chosen to be five times stronger and ten times weaker, respectively. For the case of strong repulsion, the number of steps present is small and, as might be expected, distributes itself more uniformly across the facet. Conversely, for the case of weak repulsion, many steps are generated and the (fast) first step tends to push the entire bunch toward the center of the facet. On the other hand, the number density of steps here becomes large and thus invalidates our basic assumption that the facet is macroscopically flat. A proper treatment of this regime requires a more sophisticated analysis.

IV. SUMMARY AND CONCLUSION

In this paper, we have addressed the question of the morphological equilibration of a facetted crystal by use of phenomenological equations of motion. The relevant atomistic kinetic processes (edge transfer, kink attachment and/or detachment, terrace hopping, and surface diffusion) were introduced progressively with special attention given to a proper treatment of the latter. Unlike all previous work, the role of individual step motion (including the effect of step-step interactions) was taken seriously. Approximate analytic results were obtained for two- and three-dimensional model crystals and compared to the work of others. Numerical results were presented for the two-dimensional case. Characteristic behavior is found when the various kinetic processes are individually rate limiting. The form of equilibration was observed to depend on the numerical value of an effective length $L_{\mathcal{H}}$ (compared to crystal dimensions) which depends upon the kinetic rate constants. Although each facet remains flat on macroscopic scales, multiple-step generation leads to interesting microscopic step distributions and equilibration scenarios. The latter might be observable by electron and scanning tunneling microscopies.

The principal limitation of the present work was the (self-imposed) restriction to a crystal exhibiting only two crystallographically inequivalent facets. Although generalization to include additional facets is possible in principle, it is not straightforward within our phenomenological approach. Computer simulation of lattice models (beyond nearest-neighbor interactions) is ideally suited to deal with this particular problem. On the other hand, they are not easily adapted to treat long-range step repulsion effects of the sort considered herein. We conclude that there is considerable room for further theoretical development.

ACKNOWLEDGMENTS

The authors acknowledge valuable conversations with John Cahn, Ronald Fox, and Craig Rottman. Support for this work was provided by the U.S. Department of Energy under Grant No. DE-FG05-88ER45369.

APPENDIX

As discussed by Mullins[11] in the context of a nearest-neighbor bond-breaking model on a square lattice in two dimensions, the surface energy

$$\gamma(\theta)=\gamma_0(\cos\theta+\sin\theta) \quad 0<\theta<\pi/2 \tag{A1}$$

repeated symmetrically in all four quadrants of the polar angle θ leads trivially to a square equilibrium crystal shape with (in our notation) $\gamma_1=\gamma_2=\gamma_0$. In that case, Gibbs's formula[15] for the average chemical potential beneath each flat facet reduces exactly to (48).

Now consider the introduction of steps onto such a facet such that the surface is inclined from perfect flatness by only a small angle θ. The surface energy per unit (projected) area of the flat surface now takes the form[12,13]

$$f(\theta)=\gamma(\theta)\sqrt{1+\tan^2\theta}\simeq\gamma_0+\gamma_0|\theta|+g|\theta|^3+\cdots, \tag{A2}$$

where the cubic term ($g>0$) arises in part from an amendment to (63) which takes account of step-step interactions of the form described by the quantity $\mu^i(s)$ in (28). The effect of these interactions on the equilibrium crystal shape is well known.[33] If the point $x=z=0$ denotes the center of the two-dimensional crystal, the top surface profile is

$$z(x)=\begin{cases} z_0, & |x|<x_0 \\ z_0-(2/3^{3/2})(\Delta p/g)^{1/2}(x-x_0)^{3/2}, & |x|>x_0 \end{cases}, \tag{A3}$$

where $x_0=z_0=\gamma_0/\Delta p$ and Δp is the pressure difference between the crystal and the medium with which it is in equilibrium. From equilibrium thermodynamics,[8,15] the latter is precisely equal to $2\gamma_0/l_e$ in our case, so that the crystal begins to curve away from the flat facet at $x_0=l_e/2$, i.e., just at the corner. Thus, the equilibrium crystal shape remains a square.

[1]G. Wulff, Z. Kristall. Miner. **34**, 449 (1901).

[2]L. V. Mikheev and V. L. Pokrovsky, J. Phys. I **1**, 373 (1991).

[3]For a review, see J. J. Metois and J. C. Heyraud, Ultramicroscopy **31**, 73 (1989).

[4]See, e.g., the various contributions to *Kinetics of Ordering and Growth at Surfaces,* edited by M. G. Lagally (Plenum, New York, 1990).

[5]R. M. Aikin and M. R. Plichta, Acta Metall. **38**, 77 (1990), and references therein.

[6]G. J. Shiflet, H. I. Aaronson, and T. H. Courtney, Scr. Metall. **11**, 677 (1977).

[7]J. M. Bermond and J. A. Venables, J. Cryst. Growth **64**, 239 (1983).

[8]R. Kern, in *Morphology of Crystals,* edited by I. Sunagawa (Terra Scientific, Tokyo, 1987), Part A, pp. 77–206.

[9]S. H. Yu and S. A. Hackney, Scr. Metall. **24**, 2077 (1990).

[10]H. van Beijeren and I. Nolden, in *Structure and Dynamics of Surfaces II,* edited by W. Schommers and P. von Blanckenhagen (Springer, Berlin, 1987), pp. 259–300.

[11]W. W. Mullins, in *Metal Surfaces,* edited by W. D. Robertson and N. A. Gjostein (American Society for Metals, Metals Park, 1963), pp. 17–66.

[12]A. Rettori and J. Villain, J. Phys. (Paris) **49**, 257 (1988).

[13]M. Ozdemir and A. Zangwill, Phys. Rev. B **42**, 5013 (1990).

[14]J. Keizer, *Statistical Thermodynamics of Nonequilibrium Processes* (Springer-Verlag, New York, 1987).

[15]J. W. Gibbs, *The Collected Works of J. Willard Gibbs* (Yale University Press, New Haven, 1948), Volume I, pp. 55–349. See also C. Herring, in *The Physics of Powder Metallurgy,* edited by W. E. Kingston (McGraw-Hill, New York, 1951), pp. 143–179.

[16]Cahn and Hoffman [J. W. Cahn and D. W. Hoffman, Acta Metall. **22**, 1205 (1974); D. W. Hoffman and J. W. Cahn, Surf. Sci. **31**, 368 (1972)] argue that it is possible to compute the value of the chemical potential at any point on a facet and the authors of Ref. 9 attempt to do so in their study of the morphological equilibration problem. The approximate nature of the latter is discussed in Sec. III. In the present paper, we do not attempt any such refinements.

[17]Even in equilibrium, steps will be present on any macroscopic facet.

[18]In writing these formulas, we have presumed that $(1/A)dN/dt \approx d/dt(N/A)$. One can verify that our final solution is consistent with this approximation. The corrections are $O(1/l)$ and smaller.

[19]T. L. Hill, *An Introduction to Statistical Thermodynamics* (Dover, New York, 1986).

[20]This is the so-called "quantum concentration," $n_Q = 2\pi m k_B T q_z h^{-2}$, where m is the adatom mass, h is Planck's constant, and q_z is the partition function of an adatom vibrating normal to the facet surface. We shall ignore the fact that q_z may be slightly different on inequivalent facets.

[21]Note that this does *not* imply that $\gamma_1 = \gamma_2$.

[22]The fact that $\Lambda_{12} = \Lambda_{21}$ is a central feature of the kinetic formulation of Ref. 14. The correctness of our assignment of the quantity Λ [defined above (5)] to their common value is *not* obvious at this point but will become so presently. The same remark applies ot other uses of previously defined rate constants later in the paper.

[23]As noted earlier, the basic driving force for mass transfer is the facet-size dependence of the equilibrium adatom concentrations as expressed in (18). This point was overlooked by Bermond and Venables (Ref. 7). Instead, the chemical potential imbalance is inserted by hand [Eq. (15) in Ref. 7] in a manner that they themselves label "arbitrary." The correct result is obtained only in the linear regime.

[24]W. K. Burton, N. Cabrera, and F. C. Frank, Philos. Trans. R. Soc. A **243**, 299 (1951).

[25]A. F. Andreev and Yu. A. Kosevich, Zh. Eksp. Teor. Fiz. **81**, 153 (1981) [Sov. Phys.—JETP **54**, 761 (1981)].

[26]E. E. Gruber and W. W. Mullins, J. Phys. Chem. Solids **28**, 875 (1967).

[27]A slightly different expression for $\mu^i(s)$ is appropriate for steps that bound local maxima or minima in the microscopic facet profile. See Refs. 12 and 13 for details.

[28]A. P. Peirce and H. Rabitz, Phys. Rev. B **38**, 1734 (1988).

[29]The difference between Λ^+ and Λ^- (which can be quite significant) has interesting physical consequences. See, e.g., G. S. Bales and A. Zangwill, Phys. Rev. B **41**, 5500 (1990).

[30]See the footnote on page 325 of Ref. 15.

[31]R. Ghez, *A Primer of Diffusion Problems* (Wiley, New York, 1988).

[32]J. P. Hirth and G. M. Pound, *Condensation and Evaporation-Nucleation and Growth Kinetics* (Pergamon, Oxford, 1963).

[33]J. J. Sáenz and N. Garcia, Surf. Sci. **155**, 24 (1985).

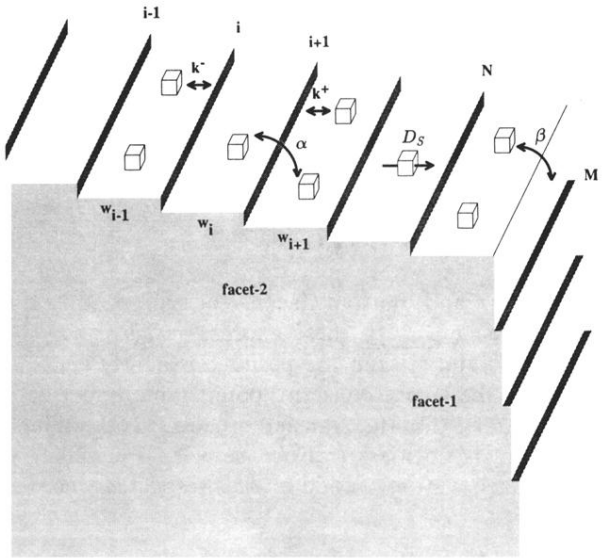

FIG. 2. An expanded view of a convex (exterior) corner of the parallelepiped shown in Fig. 1 which reveals the step structure of the facets. Although shown as straight, the step edges should be regarded as densely populated by kinks. The kinetic processes depicted are surface diffusion (D_S), exchange of atoms between terrace sites at an "up step" (k^+), exchange of atoms between terrace sites at a "down step" (k^-), exchange of adatoms between terraces on the *same* facet (α), and exchange of adatoms between terraces on *adjacent* facets (β).